Theoretical investigations on the molecular structure, vibrational spectra, HOMO–LUMO and NBO analysis of 5-chloro-2-((4-chlorophenoxy)methyl)benzimidazole

ARTICLE *in* SPECTROCHIMICA ACTA PART A MOLECULAR AND BIOMOLECULAR SPECTROSCOPY · NOVEMBER 2013

Impact Factor: 2.35 · DOI: 10.1016/j.saa.2013.11.025 · Source: PubMed

Spectrochimica Acta Part A: Molecular and Biomolecular Spectroscopy 122 (2014) 499–511

Contents lists available at ScienceDirect

Spectrochimica Acta Part A: Molecular and Biomolecular Spectroscopy

journal homepage: www.elsevier.com/locate/saa

Theoretical investigations on the molecular structure, vibrational spectra, HOMO–LUMO and NBO analysis of 5-chloro-2-((4-chlorophenoxy)methyl)benzimidazole

Y. Shyma Mary [a,b,*], P.J. Jojo [b], C. Yohannan Panicker [c], Christian Van Alsenoy [d], Sanaz Ataei [e], Ilkay Yildiz [f]

[a] Department of Physics, Bharathiar University, Coimbatore, Tamil Nadu, India
[b] Department of Physics, Fatima Mata National College, Kollam, Kerala, India
[c] Department of Physics, TKM College of Arts and Science, Kollam, Kerala, India
[d] Department of Chemistry, University of Antwerp, B2610 Antwerp, Belgium
[e] Ankara University, Institute of Biotechnology, 06100 Tandogan, Ankara, Turkey
[f] Ankara University, Faculty of Pharmacy, Department of Pharmaceutical Chemistry, 06100 Tandogan, Ankara, Turkey

HIGHLIGHTS

- IR, Raman spectra and NBO analysis were reported.
- The wavenumbers are calculated theoretically using Gaussian09 software.
- The wavenumbers are assigned using PED analysis.
- The geometrical parameters are in agreement with that of similar compounds.

GRAPHICAL ABSTRACT

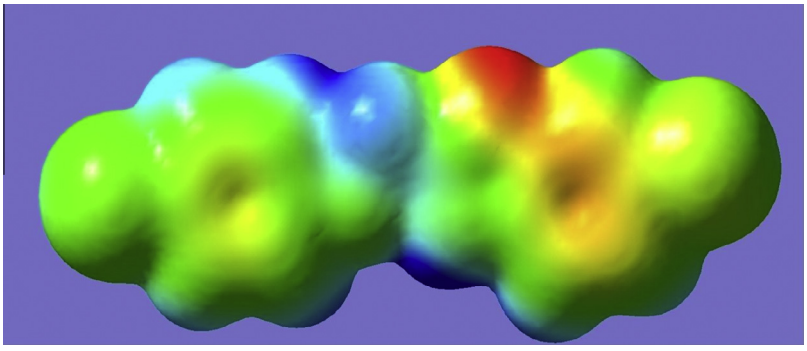

ARTICLE INFO

Article history:
Received 17 October 2013
Received in revised form 3 November 2013
Accepted 5 November 2013
Available online 14 November 2013

Keywords:
FT-IR
FT-Raman
Benzimidazole
Hyperpolarizability
PED

ABSTRACT

The optimized molecular structure, vibrational frequencies, corresponding vibrational assignments of 5-chloro-2-((4-chlorophenoxy)methyl)benzimidazole have been investigated experimentally and theoretically using Gaussian09 software package. The energy and oscillator strength calculated by time dependent density functional theory results almost compliments with experimental findings. Gauge-including atomic orbital ^{1}H NMR chemical shifts calculations were carried out and compared with experimental data. The HOMO and LUMO analysis is used to determine the charge transfer within the molecule. The stability of the molecule arising from hyper-conjugative interaction and charge delocalization has been analyzed using NBO analysis. Molecular electrostatic potential was performed by the DFT method and the infrared intensities and Raman activities are reported. Mulliken's net charges have been calculated and compared with the atomic natural charges. Fist hyperpolarizability is calculated in order to find its role in non-linear optics.

Introduction

Benzimidazole derivatives possess a variety of biological activities and pharmacological effects. Several compounds containing benzimidazole group, have been reported to exhibit antimicrobial [1–3], anticancer [4,5], antifungal [6,7], anti-parasitic [8], antiviral

* Corresponding author at: Department of Physics, Bharathiar University, Coimbatore, Tamil Nadu, India. Tel.: +91 9895370968.
E-mail address: yshymamary@rediffmail.com (Y.S. Mary).

1386-1425/$ - see front matter © 2013 Elsevier B.V. All rights reserved.
http://dx.doi.org/10.1016/j.saa.2013.11.025

[9] and anti-inflammatory [10] activities. Benzimidazole and its derivatives show pharmaceutical activity [11–17], such as lowering of blood sugar level, inhibition of phosphodiesterase-5 [18], as well as casein kinase-2 and -5 [19]. Despite a numerous attempts to develop new structural prototype in the search for more effective antimicrobials, the benzimidazoles still remain as one of the most versatile class of compounds against microbes [20–27] and, therefore, are useful substructures for further molecular exploration. Benzimidazole-containing heterocyclic moieties have found extensive uses in agriculture [28]. The benzimidazole scaffold is an accepted pharmacophore and represents an important synthetic precursor in new drug discovery [29–36]. Yildiz-Oren et al. [37] synthesized 5-chloro-2-((4-chlorophenoxy)methyl)benzimidazole for evaluating microbiological activity. The minimum inhibitory concentrations (MIC) of the title compound against *Staphylococcus aureus*, *Streptococcus faecalis*, *Bacillus subtilis* as Gram-positive and *Escherichia coli*, *Klebsiella pneumoniae*, *Pseudomonas aeruginosa* as Gram negative bacteria and *Candida albicans* as a yeast were obtained by using twofold serial dilution technique and compared to ampicillin, amoxycillin, tetracycline, streptomycin, clotrimazole and haloprogin as standard drugs. According to this study, the title structure was found to be moderately potent against *S. aureus*, *S. faecalis*, *B. subtilis*, *E. coli*, *K. pneumonia*, *P. aeruginosa*, *C. albicans* (MIC values of 50, 50, 25, 50, 25, 25, 12.5 μg/mL, respectively). Besides, this compound showed more potent than the standard drug streptomycin against *S. faecalis* and *B. subtilis*. Moreover, 5-chloro-2-((4-chlorophenoxy)methyl)benzimidazole exhibited significant antibacterial activity with MIC values of 25 μg/mL for the Gram-negative enterobacter *P. aeruginosa*, which is effective in nosocomial infections and often resistant to antibiotic therapy, providing higher potencies than the compared standard drugs. Considering the enormous biological importance, 5-chloro-2-((4-chlorophenoxy)methyl)benzimidazole is re-synthesized and the detailed experimental and theoretical normal Raman spectroscopy, and FTIR spectra are reported in the present work.

Experimental details

The title compound was prepared involving the reaction of 4-chloro-2-phenylenediamine with 4-chloro-phenoxyacetic acid in the presence of dehydrating agents in one step procedure as shown in 'Scheme 1' [37]. During the synthesis of 5-chloro-2-((4-chlorophenoxy)methyl)benzimidazole aqueous hydrochloric acid was used as the condensation reagent according to well-known Philips' method [38]. A mixture of 4-chloro-phenoxyacetic acid (10 mmol) and 4-chloro-2-phenylenediamine (10 mmol) was boiled under reflux with stirring for 19 h in 15 ml 6 N HCl. At the end of the reaction period, the mixture was neutralized with excess of $NaHCO_3$. The collected precipitate washed with water, dried in vacuum, purified by flash chromatography, eluting with $CHCl_3$ and recrystallized by using EtOH-H_2O. m.p: 182–183 °C [37], Yield 35%, Reaction temperature 100 °C, Elemental analysis: C% 57.33 (Calculated) 57.53 (Found); H% 3.41 (Calculated) 3.40 (Found); N% 9.55 (Calculated) 9.51 (Found).

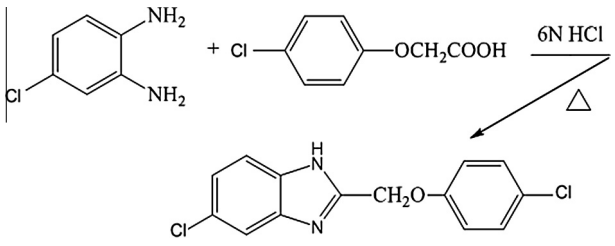

Scheme 1. Synthetic pathway of the title compound.

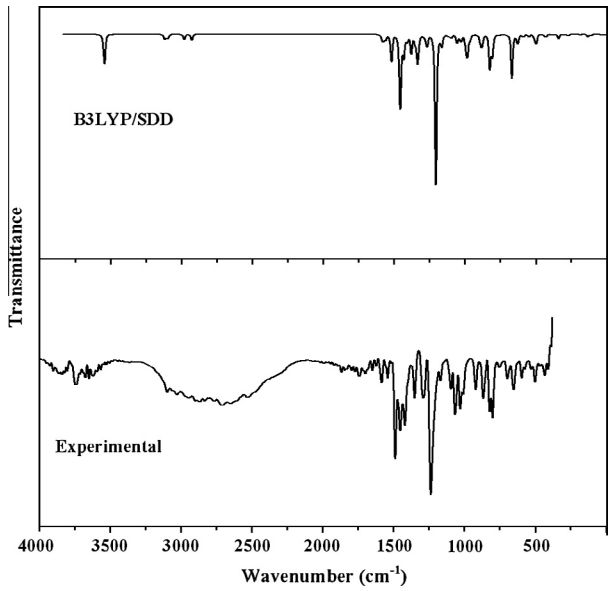

Fig. 1. FT-IR spectrum of 5-chloro-2-((4-chlorophenoxy)methyl)benzimidazole.

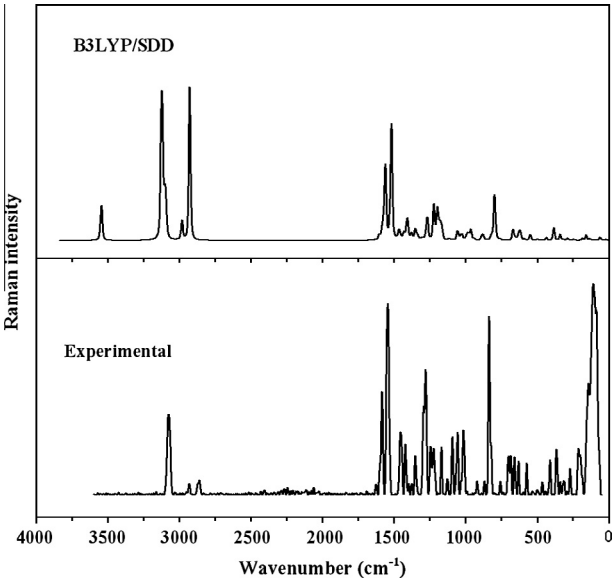

Fig. 2. FT-Raman spectrum of 5-chloro-2-((4-chlorophenoxy)methyl)benzimidazole.

The FT-IR spectrum (Fig. 1) was recorded using KBr pellets on a DR/Jasco FT-IR 6300 spectrometer. The FT-Raman spectrum (Fig. 2) was obtained on a Bruker RFS 100/s, Germany. For excitation of the spectrum the emission of Nd:YAG laser was used, excitation wavelength 1064 nm, maximal power 150mW, measurement on solid sample. ^1H NMR spectra were obtained with a Bruker AC 80 MHz spectrometer and TMS was used as an internal standard. Elemental analyses were carried out with a Perkin–Elmer model 240-C apparatus.

Computational details

Calculations of the title compound are carried out with Gaussian09 program [39] using the HF/6-31G*, B3LYP/6-31G* and

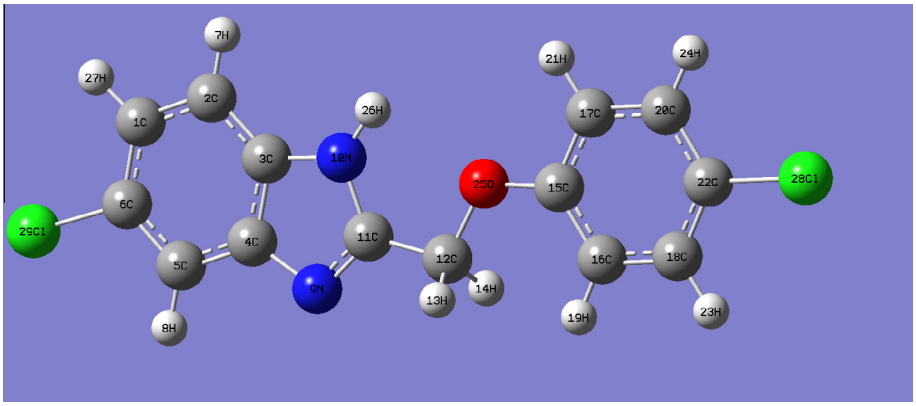

Fig. 3. Optimized geometry (SDD) of 5-chloro-2-((4-chlorophenoxy)methyl)benzimidazole.

B3LYP/SDD basis sets to predict the molecular structure and vibrational wave numbers. Molecular geometry was fully optimized by Berny's optimization algorithm using redundant internal coordinates. Harmonic vibrational wave numbers are calculated using the analytic second derivatives to confirm the convergence to minima on the potential surface. The wave number values computed at the Hartree–Fock level contain known systematic errors due to the negligence of electron correlation [40]. We therefore, have used the scaling factor value of 0.8929 for HF/6-31G* basis set. The DFT hybrid B3LYP functional and SDD methods tend to overestimate the fundamental modes; therefore scaling factor of 0.9613 has to be used for obtaining a considerably better agreement with experimental data [40]. The Stuttagart/Dresden effective core potential basis set (SDD) [41] was chosen particularly because of its advantage of doing faster calculations with relatively better accuracy and structures [42]. Then frequency calculations were employed to confirm the structure as minimum points in energy. Parameters corresponding to optimized geometry (SDD) of the title compound (Fig. 3) are given in Table S1 as supporting material. The absence of imaginary wave numbers on the calculated vibrational spectrum confirms that the structure deduced corresponds to minimum energy. The assignments of the calculated wave numbers are aided by the animation option of GAUSSVIEW program, which gives a visual presentation of the vibrational modes [43]. The potential energy distribution (PED) is calculated with the help of GAR2PED software package [44]. The ^{1}H NMR data were obtained from the DFT method using basis set 6-31G*. The characterization of excited states and electronic transitions were performed using the time-dependent DFT method (TDB3LYP) on their correspondingly optimized ground state geometries. We used the time-dependent density functional theory (TD-DFT), which is found to be an accurate method for evaluating the low-lying excited states of molecules and has been thoroughly applied to solve physical and chemical problems. Vertical excitation energies were computed for the first 30 singlet excited states, in order to reproduce the experimental electronic spectra. Potential energy surface scan studies have been carried out to understand the stability of planar and non-planar structures of the molecule. The HOMO and LUMO are calculated by B3LYP/SDD method.

Results and discussion

IR and Raman spectra

The observed IR and Raman bands and calculated (scaled) wave numbers and assignments are given in Table 1. The C═N stretching skeletal bands [45–48] are observed in the range 1650–1500 cm^{-1}. For the title compound, the SDD calculations give υC═N mode at 1520 cm^{-1} with a band at 1518 cm^{-1} in the IR spectrum. Similar values are reported at 1536 cm^{-1} for 5-nitro-2-(4-nitrobenzyl)benzoxazole [49].

Primary aromatic amines with nitrogen directly on the ring absorb strongly at 1330–1260 cm^{-1} due to stretching of the phenyl carbon–nitrogen bond [50]. Sandhyarani et al. [51] reported υCN at 1318 cm^{-1} for 2-mercaptobenzothiazole. For the title compound υCN is assigned at 1333, 1199, 1177 cm^{-1} theoretically (SDD). These modes are not pure but contain a significant contribution from other modes. For 5-nitro-2-(4-nitrobenzyl) benzoxazole C—N stretching vibrations are observed in the region 1228–1195 cm^{-1} [49]. CN stretching modes are reported at 1268, 1220, 1151 cm^{-1} theoretically for benzimidazolium salts by Malek et al. [52].

In aromatic compounds the υNH appears the region 3400 ± 40 cm^{-1} [53]. The SDD calculations give a value of 3544 cm^{-1} for this υNH mode and a band is observed in the IR spectrum at 3548 cm^{-1} and at 3424 cm^{-1} in the Raman spectrum. N—H group show bands at 1510–1500, 1400–1300 and 740–730 cm^{-1} [54]. According to literature, if N—H is a part of a closed ring [54,55] the C—N—H deformation band is absent in the region 1510–1500 cm^{-1}. For the title compound the C—N—H deformation band assigned at 1409 cm^{-1} theoretically (SDD). The out of plane NH deformation is expected in the region 650 ± 50 cm^{-1} [53] and the band at 660 cm^{-1} in the Raman spectrum and at 669 cm^{-1} theoretically (SDD) are assigned as this mode. Minitha et al. [56] reported υNH at 3469 cm^{-1}, δNH at 1300 cm^{-1} and γNH at 535 cm^{-1}. Panicker et al. reported the out-of-plane bending mode of NH at 746 cm^{-1}, theoretically [57]. Kim et al. reported [58] NH deformation bands at 549, 1484 cm^{-1} in the Raman spectrum and at 556, 1495 cm^{-1} theoretically for benzimidazole and Malek et al. [52] reported modes at 1394, 680 cm^{-1} theoretically as NH deformation.

The vibrations of the CH_2 group, the asymmetric stretch $\upsilon_{as}CH_2$, symmetric stretch υ_sCH_2, scissoring vibration δCH2, appear in the region 2945 ± 45, 2885 ± 45 and 1445 ± 35 cm^{-1}, respectively [50,53]. The SDD calculations give $\upsilon_{as}CH_2$ at 2982 cm^{-1} and υ_sCH_2 at 2928 cm^{-1}. The bands observed at 2974, 2931 cm^{-1} (Raman) and 2940 cm^{-1} (IR) are assigned as the stretching modes of CH_2 group. In the present case, the band observed at 1454 cm^{-1} in the IR, 1456 cm^{-1} in the Raman spectrum and 1456 cm^{-1} (SDD) are assigned as the scissoring mode of CH_2. Bands of hydrocarbons due to CH_2 twisting and wagging vibrations are observed in the region 1180–1390 cm^{-1} [47,50]. The CH_2 wagging and twisting modes are assigned at 1382 cm^{-1} and 1206 cm^{-1} theoretically (SDD). The band calculated at 966 cm^{-1} is assigned as the rocking mode of CH_2.

Table 1
Vibrational assignments of 5-chloro-2-((4-chlorophenoxy)methyl)benzimidazole.

HF/6-31G*			B3LYP/6-31G*			B3LYP/SDD			IR	Raman	Assignments
υ	IR_I	R_A	υ	IR_I	R_A	υ	IR_I	R_A	υ	υ	–
3524	145.14	67.74	3355	96.39	102.11	3544	109.10	104.02	3548	3424	υNH(99)
3058	0.22	76.46	3133	0.12	83.42	3126	0.26	88.09	–	3163	υCHI(97)
3051	2.67	216.81	3125	2.11	221.61	3123	1.91	235.17	–	–	υCHII(99)
3049	4.75	13.84	3122	4.43	21.16	3119	6.96	3.07	–	–	υCHII(99)
3046	3.82	120.52	3121	3.25	131.41	3118	4.57	113.62	–	–	υCHI(97)
3035	0.25	85.21	3109	4.36	69.78	3103	6.89	46.90	–	–	υCHII(98)
3034	8.45	8.32	3106	5.73	31.26	3102	4.92	35.72	3097	–	υCHII(98)
3021	4.27	61.59	3094	5.51	68.85	3092	4.26	51.44	3031	3076	υCHI(99)
2928	14.64	50.49	2966	16.09	58.15	2982	16.89	44.39	2940	2974	υCH_2(100)
2880	7.19	142.46	2923	10.88	277.86	2928	16.33	296.68	–	2931	υCH_2(100)
1635	5.56	5.06	1614	0.24	6.01	1605	0.47	5.91	1622	1626	υPhI(56), υPhII(23)
1613	37.86	22.80	1591	19.78	18.09	1582	27.94	24.10	1584	1584	υPhII(67), δCHII(13)
1596	10.46	15.42	1578	19.03	37.37	1565	16.87	50.87	–	–	υPhII(60)
1591	9.32	38.87	1571	8.04	70.94	1561	5.02	73.10	1542	1544	υPhI(65)
1569	143.45	132.51 1529	98.91	181.82	1520	94.89	192.10	1518	–		υPhI(18)
1505	183.16	3.18	1493	47.05	20.44	1468	29.20	14.48	1489	–	υPhII(62), δCHII(11)
1490	60.11	10.49	1482	156.91	14.87	1456	218.66	5.19	1454	1456	δCH_2(45), δCHII(15), υPhII(16)
1466	77.18	6.47	1452	61.26	9.80	1433	75.72	11.65	1420	1422	υPhI(41), δCHI(20)
1446	27.64	18.46	1427	16.59	47.25	1409	26.92	45.93	–	–	δNH(59), υPhI(26)
1407	21.37	1.33	1401	5.53	1.16	1382	8.97	2.06	–	1398	δCH_2(55), υPhII(42)
1405	87.32	5.30	1387	71.65	11.31	1379	50.78	8.23	–	1375	υPhI(53), υCN(13), δCHI(12)
1363	142.15	6.97	1359	20.32	25.23	1351	33.04	21.67	1352	1353	δCHI(26), υPhI(61)
1328	65.44	16.54	1339	116.65	9.59	1333	113.51	5.92	–	–	υCN(61), υPhII(10)
1318	7.45	4.88	1309	0.19	2.99	1305	1.93	3.42	–	1296	υPhII(79)
1253	245.14	30.09	1309	2.01	1.61	1285	4.83	1.30	1292	1280	δCHII(87)
1249	122.78	6.39	1283	40.25	27.56	1270	45.78	41.13	–	1255	υCN(15), υPh I(22), δCHI(40)
1242	113.62	56.73	1236	9.31	34.01	1223	7.41	44.49	1237	1225	δCHI(47), υCN(15)
1227	6.16	12.38	1221	440.51	4.80	1206	411.48	5.4	–	–	δCH_2(45)
1209	8.24	13.64	1205	28.35	53.51	1199	48.92	31.82	–	–	υPhI(10), δCHI(10), υCN(50)
1196	78.55	0.94	1194	3.22	14.56	1191	1.62	12.10	–	1193	υCOC(67)
1189	5.63	21.25	1185	17.45	23.55	1177	4.75	30.38	–	–	υCN(58), δPhI(21)
1180	10.48	6.62	1179	31.59	14.97	1165	37.50	10.40	1169	1170	δCHII(71)
1133	2.56	6.30	1133	3.46	3.07	1115	5.02	2.86	–	1120	δCHI(52), υPhI(15)
1104	11.08	0.04	1112	9.86	0.53	1098	13.80	0.70	1095	1093	δCHII(60), υPhII(27)
1073	25.14	8.79	1068	43.69	16.51	1056	35.93	18.26	1066	1056	υPhII(36), δCHII(12)
1046	34.52	7.04	1039	32.72	10.69	1029	29.51	12.02	1030	1033	υPhI(50), δCHI(27)
1038	0.11	1.52	1023	0.04	0.99	1013	0.05	0.45	1008	1016	δCHII(83)
1032	82.79	3.96	1005	4.39	0.74	993	65.30	9.67	–	992	υCOC(54)
1030	0.03	0.31	999	105.71	14.37	982	47.17	5.09	–	–	δPhI(53), υPhII(22)
1020	0.01	1.21	978	32.05	13.98	966	16.50	16.20	–	–	δRingII(23), δCH_2(63)
1018	0.20	0.11	955	0.01	0.47	958	0.15	0.13	–	–	γCHII(89)
1009	59.09	3.13	943	0.08	1.50	942	0.88	2.54	–	951	γCHI(87)
993	7.20	29.24	939	0.03	0.11	939	0.12	0.58	921	938	γCHII(78), τPhII(18)
964	24.36	0.07	895	52.53	10.24	891	23.71	1.88	–	–	γCHI(76), τPhI(14)
901	59.64	16.87	889	19.57	0.71	882	49.50	10.72	868	889	δPh I(26), υCCl (56)

Table 1 (*continued*)

HF/6-31G*			B3LYP/6-31G*			B3LYP/SDD			IR	Raman	Assignments
υ	IR_I	R_A	υ	IR_I	R_A	υ	IR_I	R_A	υ	υ	–
879	126.85	0.86	829	4.85	3.54	826	96.06	0.72	823	837	γCHII(23), υPhII(42), γCOC(12)
861	6.61	1.85	826	79.31	0.98	820	5.11	6.30	–	823	γCHII(53), υCN(15)
858	57.57	1.93	812	3.02	59.69	809	10.64	0.03	–	–	γCHII(97)
829	16.06	4.10	808	9.20	3.24	807	54.41	0.81	802	–	γCHI(74)
814	2.05	56.92	804	42.94	2.49	798	4.02	61.97	–	799	υCCl(38), δPhII(20), δCCO(11)
783	0.71	2.09	743	0.68	2.32	759	2.75	1.41	755	758	τPhI(50), τRingIII(33)
732	2.83	0.38	721	1.59	0.24	710	0.72	0.10	–	704	δRingIII(26), δPhII(13), δPhI(12)
721	3.37	0.17	696	0.07	0.19	693	0.48	0.11	699	685	τPhII(69), γCOC(15), γCCl(10)
694	105.13	4.19	679	29.66	9.69	669	104.36	0.34	–	660	γNH(97)
682	35.62	10.53	654	57.71	2.52	669	27.27	13.29	–	660	δRingIII(31), δPhI(27), υCCl(19)
659	57.54	0.57	649	76.59	0.41	655	0.85	2.02	653	–	τRingIII(54), γCC(24)
643	32.70	12.81	641	38.94	8.04	630	36.43	10.81	–	631	δPhII(31), υCCl(22), δRingIII(26)
638	1.79	6.56	634	0.03	6.18	620	0.19	8.98	–	–	δPhII(81)
621	29.04	1.27	593	6.40	1.19	588	10.55	2.10	596	574	γCCl(10), τPhI(52), τRingIII(11)
556	9.43	5.04	558	8.55	5.15	551	6.57	6.92	534	535	δPhI(36), δRingIII(16), δCCl(15)
525	17.47	0.75	515	19.16	1.04	509	18.67	0.60	502	522	δCC(22), δPh I(21), δCOC(21)
516	18.37	0.43	502	12.25	0.62	497	22.19	1.19	500	–	τPhII(36), γCOC(31), γCCl(23)
448	7.86	0.52	443	1.86	2.71	438	2.07	3.04	–	443	δCOC(43), δCCl(15)
443	1.49	5.20	429	5.18	0.52	431	9.48	0.39	434	–	τPhII(46), τRingIII(27), τPhI(12)
430	0.02	0.09	419	0.05	0.09	412	0.08	0.09	408	411	τPhII(84)
391	2.80	14.49	391	2.26	12.15	385	2.17	13.87	–	–	δCCl(24), δPhI(16), δPhII(14), δCCO(11)
364	0.29	0.13	350	0.13	0.01	352	0.01	0.02	–	367	τRingIII(24), γCC(14), τPhI(14)
346	12.73	6.90	345	14.89	5.55	340	13.09	6.13	–	339	δCCl(44), δPhI(25)
335	1.61	1.75	321	0.75	1.36	317	0.79	0.93	–	314	δC=N (39), τPhII(25), γCO(13)
295	1.65	2.47	296	1.22	2.03	291	1.50	2.39	–	292	δCCl(52), δCC(11)
284	5.66	0.64	274	4.11	0.78	274	4.34	0.62	–	271	τPhI(45), γCC(13), τRingII(13), γCCl(10)
249	0.59	1.67	248	0.43	1.28	244	0.52	1.43	–	213	δCCl(67)
186	0.76	2.46	183	0.93	2.67	186	1.34	2.05	–	–	τPhI(34), γCC(13), τRingIII(21)
159	0.03	4.16	161	0.04	4.42	160	0.04	4.93	–	–	δCCl(33), δCCO(20)
136	5.97	0.02	134	1.75	1.32	133	1.78	1.49	–	138	δCOC(46), δCC(16), δCCl(10)

(*continued on next page*)

Table 1 (*continued*)

HF/6-31G*			B3LYP/6-31G*			B3LYP/SDD			IR	Raman	Assignments
υ	IR_I	R_A	υ	IR_I	R_A	υ	IR_I	R_A	υ	υ	–
132	1.85	1.34	133	4.18	0.12	133	4.57	0.21	–	–	τCCO(44), τPhII(27), γCCl(10)
107	7.87	0.89	106	5.41	0.84	112	6.03	0.79	–	110	τCCO(28), τPhI(16), γCCl(11), τRingIII(10)
55	0.19	4.37	59	0.01	4.52	62	0.06	4.02	–	–	τCCO(54), τRingIII(10)
39	1.54	0.05	40	1.46	0.09	39	1.34	0.09	–	–	δCCO(31), δCOC(32), δCC(25)
20	0.49	1.03	18	0.12	0.65	20	0.56	0.63	–	–	τCCO(66), γCC(18)
12	3.70	0.57	11	4.17	1.12	16	3.38	0.59	–	–	τCCO(78), γNH(15)

υ – stretching; δ – in-plane deformation; γ – out-of-plane deformation; τ – torsion; PhI – tri-substituted benzene ring; PhII – para substituted benzene ring; RingIII – benzimidazole ring; IR_I – IR intensity; R_A – Raman activity; PED contribution in% is given in brackets in the assignment column.

For the title compound, as expected the asymmetric C—O—C stretching vibration is assigned at 1191 cm^{-1} and the symmetric stretching mode at 993 cm^{-1} (SDD) theoretically [47]. The C—O—C stretching modes are reported at 1250 and 1073 cm^{-1} for 2-mercpatobenzoxazole [59]. Bhagyasree et al. [49] reported C—O—C stretching modes at 1144, 1063 (IR), 1146, 1066 (Raman) and at 1153, 1079 cm^{-1} theoretically (SDD).

The vibrations belonging to the bond between the ring and chlorine atoms are worth to discuss here since mixing of vibrations is possible due to the lowering of the molecular symmetry and the presence of heavy atoms on the periphery of the molecule [60]. Mooney [61,62] assigned vibrations of C—Cl, Br, and I in the wave number range of 1129–480 cm^{-1}. The CCl stretching vibrations give generally strong bands in the region 710–505 cm^{-1}. For simple organic chlorine compounds, CCl absorptions are in the region 750–700 cm^{-1}. Sundaraganesan et al. [63] reported CCl stretching at 704 (IR), 705 (Raman), and 715 cm^{-1} (DFT) and the deformation bands at 250 and 160 cm^{-1}. The aliphatic CCl absorb [53] in the range 830–560 cm^{-1} and putting more than one chlorine atom on a carbon atom raises the CCl wave number. The CCl_2 stretching modes are reported at 738 and 284 cm^{-1} for dichloromethane [50,64]. Pazdera et al. [65,66] reported the CCl stretching mode at 890 cm^{-1}. For 2-cyanophenylisocyanide dichloride, the CCl stretching mode is reported at 870 cm^{-1} in the IR spectrum, 877 cm^{-1} in the Raman spectrum and at 882 cm^{-1} theoretically [67]. Arslan et al. [68] reported the CCl stretching mode at 683 (experimental), and at 711, 736, 687, 697 cm^{-1} theoretically. The deformation bands of CCl are reported [68] at 431, 435, 441, and 441 cm^{-1}. For the title compound, the bands at 868 cm^{-1} in the IR, 889, 799 cm^{-1} in Raman and 882, 798 (SDD) are assigned as CCl stretching modes. The deformation bands of CCl are also identified. This is in agreement with the literature data [64,69,70]. For 4-chlorophenylboronic acid, the CCl stretching and deformation bands are reported at 571 (DFT), and at 287 and 236 cm^{-1}, respectively [71].

Since the identification of all the normal modes of vibration of large molecules is not trivial, we tried to simplify the problem by considering each molecule as substituted benzene. Such an idea has already been successfully utilized by several workers for the vibrational assignments of molecules containing multiple homo and hetero aromatic rings [72–76]. In the following discussion, the tri-substituted and para substituted phenyl rings are designated as rings PhI and PhII, respectively and benzimidazole as ringIII. The modes in the two phenyl rings will differ in wave number and the magnitude of splitting will depend on the strength of interactions between different parts (internal coordinates) of the two rings. For some modes, this splitting is so small that they may be considered as quasi-degenerate and for the other modes a significant amount of splitting is observed. Such observations have already been reported [72–76].

The existence of one or more aromatic rings in a structure is normally readily determined from the C—H and C=C—C ring related vibrations. The C—H stretching occurs above 3000 cm^{-1} and is typically exhibited as a multiplicity of weak to moderate bands, compared with the aliphatic C—H stretch [77]. In the present case, the SDD calculations give υC—H modes in the range of 3126–3092 cm^{-1}. The bands observed at 3097, 3031 cm^{-1} in the IR spectrum and at 3163, 3076 cm^{-1} in the Raman spectrum are assigned as the υC—H modes of the benzene rings.

The benzene ring possesses six ring stretching vibrations, of which the four with the highest wave numbers (occurring respectively near 1600, 1580, 1490 and 1440 cm^{-1}) are good group vibrations. In the absence of ring conjugation, the band near 1580 cm^{-1} is usually weaker than that at 1600 cm^{-1}. The fifth ring stretching vibration is active near 1355 ± 35 cm^{-1}, a region which overlaps strongly with that of the CH in-plane deformation and the intensity is in general, low or medium [53,64]. The sixth ring stretching vibration or ring breathing mode appears as a weak band near 1000 cm^{-1} in mono-substituted benzenes [53].

For the title compound, the bands observed at 1622, 1542, 1420, 1352 cm^{-1} in the IR and 1626, 1544, 1422, 1375, 1353 cm^{-1} in the Raman spectrum are assigned as υPhI modes with 1605, 1561, 1433, 1379, 1270, 1351 cm^{-1} as SDD values. For the title compound, PED analysis gives the ring breathing mode of PhI at 1029 cm^{-1}[78]. For the phenyl ring PhI, the bands observed at 1237 cm^{-1} in the IR spectrum and at 1255, 1225, 1120 cm^{-1} in the Raman spectrum are assigned as in-plane CH deformation modes. Also SDD calculations give these modes at 1270, 1223, 1115 cm^{-1} which are in agreement with literature [78].

For para substituted benzenes, the δCH modes are seen in the range 995–1315 cm^{-1} [53]. Bands observed at 1292, 1169, 1095, 1008 cm^{-1} in the IR spectrum and at 1280, 1170, 1093, 1016 cm^{-1} in the Raman spectrum are assigned as δCH modes for the ring PhII. The corresponding theoretical values (SDD) are 1285, 1165, 1098 and 1013 cm^{-1}. For the para substituted diheavy phenyl ring, the ring stretching modes υPh modes are expected in the range 1280–1620 cm^{-1} [53]. In this case υPhII modes are assigned at 1582, 1565, 1468, 1382, 1305 cm^{-1}

theoretically and observed at 1584, 1489 cm^{-1} in IR spectrum and at 1584, 1398, 1296 cm^{-1} in Raman spectrum. The ring breathing modes for the para di-substituted benzenes with entirely different substituent [64] have been reported to be strongly IR active with typical bands in the interval 740–840 cm^{-1}. For the title compound, the ring breathing mode is assigned at 823 cm^{-1} in the IR spectrum which finds support from the theoretical value 826 cm^{-1} which has high infrared intensity. Ambujakshan et al. [79] reported a value 792 cm^{-1} (IR) and 782 cm^{-1} (HF) as ring breathing mode.

The C—H out-of-plane deformations are observed between 1000 and 700 cm^{-1} [53]. Generally the C—H out-of-plane deformations with the highest wave numbers have a weaker intensity than those absorbing at lower wave numbers. The out-of-plane γCH modes are observed at 802 cm^{-1} in the IR spectrum for PhI and at 921, 802 cm^{-1} in the IR spectrum, 938, 823 cm^{-1} in the Raman spectrum for PhII. The corresponding SDD values are 942, 891, 807 cm^{-1} for PhI and 958, 939, 820, 809 cm^{-1} for PhII. A very strong CH out-of plane deformation band, occurring at 840 ± 50 cm^{-1} is typical for 1,4-disubstituted benzenes [53]. For the title compound, a very strong γCH observed by calculation gives at 942 cm^{-1}. Again according to literature [50,53] a lower γCH absorbs in the neighborhood 820 ± 45 cm^{-1}, but is much weaker or infrared inactive and the corresponding theoretical mode is 809 cm^{-1}.

Optimized geometry

A detailed potential energy surface (PES) scan on dihedral angles C_4—N_9—C_{11}—C_{12}, N_9—C_{11}—C_{12}—O_{25}, C_{11}—C_{12}—O_{25}—C_{15} have been performed at B3LYP/6-31G(d) level to reveal all possible conformations of 5-chloro-2-((4-chlorophenoxy)methyl)-benzimidazole. The PES scan was carried out by minimizing the potential energy in all geometrical parameters by changing the torsion angle at every 10° for a 180° rotation around the bond. The results obtained in PES scan study by varying the torsion perturbation around the methyl bonds (CH_2) are given as supporting information in Figs. S1–S3. For the C_4—N_9—C_{11}—C_{12} rotation, the minimum energy was obtained at 180.0° in the potential energy curve of energy −1644.6314 Hartrees. For the N_9—C_{11}—C_{12}—O_{25} rotation, the minimum energy occurs at 180.0° in the potential energy curve of energy −1644.6313 and for C_{11}—C_{12}—O_{25}—C_{15} rotation, the minimum energy was obtained at 0.0° in the potential energy curve of energy −1644.6314 Hartrees.

To the best of our knowledge, no X-ray crystallographic data of this molecule has yet been established. The optimized molecular structure of 5-chloro-2-((4-chlorophenoxy)methyl)-benzimidazole was determined by using Gaussian09 program. From Table S1, it is clearly seen that the dihedral angles C_6—C_5—C_4—N_9 and C_4—N_9—C_{11}—C_{12}, C_1—C_2—C_3—N_{10}, C_2—C_3—N_{10}—C_{11} are 180°. This indicates that the benzene ring I and the benzimidazole ring moieties of the title compound are planar as in the case of 2-amino-6-methylbenzothiazole [80]. For 2-amino-6-methylbenzothiazole [81] the bond lengths C_4—C_5, C_4—C_3, C_3—C_2, C_4—N_9 are respectively, 1.4145, 1.4333, 1.4066, 1.4110 Å. The corresponding values for the title compound are 1.4083, 1.4311, 1.4044, 1.41 Å. The ab initio calculations give the bond angles C_3—C_4—N_9, C_4—N_9—C_{11}, C_3—N_{10}—C_{11}, N_9—C_{11}—N_{10} as 110.0°, 104.9°, 107.2° and 113.1° for the title compound. These values are in agreement with the bond angles reported for 2-amino-6-methylbenzothiazole [81] and for 2-amino-4-ethylbenzothiazole [82]. For 2-amino-4-methylbenzothiazole [82] the bond lengths C_3—C_4, C_{11}—C_{12}, C_4—N_9 are 1.3916, 1.2962, 1.4173 Å respectively.

Purkayastha and Chattopadhyay [83] reported N_9—C_{11}, N_9—C_4 bond lengths as 1.3270, 1.400 Å for benzothiazole and 1.3503, 1.407 Å for benzimidazole compounds. For the title compound we have obtained these values as 1.331 and 1.41 Å. The carbon–carbon bond lengths in the phenyl ring PhI lies between 1.3965 and 1.4152 Å while for phenyl ring PhII, the range is 1.399–1.4094 Å. The CH bond lengths lies between 1.0839 and 1.086 Å for Ph I and 1.0847–1.0855 Å for PhII. These changes in bond lengths for the title compound can be attributed to the conjugation of the phenyl ring. Here for the title compound, benzene is a regular hexagon with bond lengths somewhere in between the normal values for a single (1.54 Å) and a double (1.33 Å) bond [84].

For the title compound, the bonds C_{11}—N_9 = 1.331 Å show typical double bond characteristics. However, C_4—N_9 = 1.41, C_3—N_{10} = 1.3985, C_{11}—N_{10} = 1.3874 Å bond lengths are shorter than the normal C—N single bond length of about 1.48 Å. The shortening of the C—N bonds reveal the effects of resonance in this part of the molecule [68] and this situation can be attributed to the difference in hybridization of the different carbon atoms. The imine C_{11}=N_9 bond length is expected to be shorter than the amine C—N bond length. In the present case C_{11}—N_9 and C_{11}—N_{10} bond distances are 1.3310 and 1.3874 Å respectively. The essential skeletal angles of C_3—N_{10}—C_{11}, C_4—N_9—C_{11} are 107.2° and 104.9°. These values are particularly in excellent agreement with benizimidazole derivatives 1.316°, 1.376°, 106.2°, 105.2° [85], 1.315°, 1.387°, 106.2°, 105.2° [86]. The close proximity of the values with each other may be due to the electronic delocalization effect resulted from the super conjugation system formed in the title compound as reported in literature [87].

Lifshitz et al. [80] reported the bond lengths for N_9—C_{11}, C_3—C_2, C_4—C_5, C_3—C_4, and N_9—C_4 as 1.291, 1.374, 1.4, 1.403 and 1.401 Å. The corresponding values in the present case are 1.331, 1.4044, 1.4083, 1.4311 and 1.41 Å. Corresponding values are reported as 1.2753, 1.3492, 1.359, 1.3768, 1.3879, 1.3784, 1.3892 Å [79] and 1.2727, 1.347, 1.3594, 1.3884, 1.3777, 1.3776, 1.3903 Å [45]. The bond lengths C_4—N_9, N_9—C_{11} and C_3—C_4 are found to be 1.3436, 1.3804 and 1.3827 Å for mercaptobenzoxazole [47]. For the title compound these values are respectively, 1.41, 1.331 and 1.4311 Å. Chlorine is highly electronegative and tries to obtain additional electron density. It attempts to draw it from the neighboring atoms which moves closer together in order to share the electrons more easily as a result. Due to this the bond angles, A(1,6,5) and A(18,22,20) are found to be 123.5°, 121.5° in the present calculation, which is 120° for normal benzene. The CCl bond lengths, C_{22}—Cl_{28} = 1.8238, C_6—Cl_{29} = 1.8292 Å given by SDD calculation are in agreement with CCl bond lengths given by Madhavan et al. [74].

First hyperpolarizability

Nonlinear optics deals with the interaction of applied electromagnetic fields in various materials to generate new electromagnetic fields, altered in wavenumber, phase, or other physical properties [88]. Organic molecules able to manipulate photonic signals efficiently are of importance in technologies such as optical communication, optical computing, and dynamic image processing [89,90]. In this context, the dynamic first hyperpolarizability of the title compound is also calculated in the present study. The first hyperpolarizability (β_0) of this novel molecular system is calculated using SDD method, based on the finite field approach. In the presence of an applied electric field, the energy of a system is a function of the electric field. First hyperpolarizability is a third rank tensor that can be described by a $3 \times 3 \times 3$ matrix. The 27 components of the 3D matrix can be reduced to 10 components due to the Kleinman symmetry [91]. The components of b are defined as the coefficients in the Taylor series expansion of the energy in the external electric field. When the electric field is weak and homogeneous, this expansion becomes

$$E = E_0 - \sum_i \mu_i F^i - \frac{1}{2}\sum_{ij} \alpha_{ij} F^i F^j - \frac{1}{6}\sum_{ijk} \beta_{ijk} F^i F^j F^k - \frac{1}{24}\sum_{ijkl} \gamma_{ijkl} F^i F^j F^k F^l + \cdots$$

where E_0 is the energy of the unperturbed molecule, F^i is the field at the origin, μ_i, α_{ij}, β_{ijk} and γ_{ijkl} are the components of dipole moment, polarizability, the first hyper polarizabilities, and second hyperpolarizibilities, respectively. The calculated first hyperpolarizability of the title compound is 2.7×10^{-30} esu, which comparable with the reported values of similar derivatives [92] and which is 20.77 times that of the standard NLO material urea (0.13×10^{-30} esu) [93]. We conclude that the title compound is an attractive object for future studies of nonlinear optical properties.

NBO analysis

The natural bond orbital (NBO) calculations were performed using NBO 3.1 program [94] as implemented in the Gaussian09 package at the DFT/B3LYP level in order to understand various second-order interactions between the filled orbital of one subsystem and vacant orbital of another subsystem, which is a measure of the intermolecular de-localization or hyper conjugation. NBO analysis provides the most accurate possible 'natural Lewis structure' picture of '*j*' because all orbital details are mathematically chosen to include the highest possible percentage of the electron density. A useful aspect of the NBO method is that it gives information about interactions of both filled and virtual orbital spaces that could enhance the analysis of intra and inter molecular interactions. The second-order Fock-matrix was carried out to evaluate the donor–acceptor interactions in the NBO basis. The interactions result in a loss of occupancy from the localized NBO of the idealized Lewis structure into an empty non-Lewis orbital. For each donor (i) and acceptor (j) the stabilization energy ($E2$) associated with the delocalization $i \rightarrow j$ is determined as

$$E(2) = \Delta E_{ij} = q_i \frac{(F_{i,j})^2}{(E_j - E_i)}$$

q_i is the donor orbital occupancy; E_i, E_j the diagonal elements and F_{ij} the off diagonal NBO Fock matrix element

In NBO analysis large $E(2)$ value shows the intensive interaction between electron-donors and electron-acceptors and greater the extent of conjugation of the whole system, the possible intensive interactions are given in Table 2. The second-order perturbation theory analysis of Fock matrix in NBO basis shows strong intra molecular hyper conjugative interactions of π electrons. The intra molecular hyper conjugative interactions are formed by the orbital overlap between n (Cl) and π* (C—C) bond orbital which results in ICT causing stabilization of the system. The strong intra molecular hyper conjugative interaction of C_{18}—C_{22} from of n3(Cl_{28}) → π* (C_{18}—C_{22}) which increases ED (0.38e) that weakens the respective bonds leading to stabilization of 9.61 kcal mol^{-1}. Another intra molecular hyper conjugative interactions are formed by the orbital overlap between n(Cl) and π*(C—C) bond orbital which results in ICT causing stabilization of the system. The strong intra molecular hyper conjugative interaction of C_5—C_6 from of n3(Cl_{29}) → π* (C_5—C_6) which increases ED (0.36 e) that weakens the respective bonds leading to stabilization of 9.36 kcal mol^{-1}. Also n(N) and π* (N—C) bond orbital which results in ICT causing stabilization of the system. The strong intra molecular hyper conjugative interaction of N_{10}—C_{12} from of n1(N_{10}) → π*(N_9—C_{11}) which increases ED (0.35 e) that weakens the respective bonds leading to stabilization of 50.23 kcal mol^{-1}. These interactions are observed as an increase in electron density (ED) in C—C, N—C anti bonding orbital that weakens the respective bonds.

The increased electron density at the oxygen atom leads to the elongation of respective bond length and a lowering of the corresponding stretching wavenumber. The electron density (ED) is transferred from the n(Cl), n(N) to the anti-bonding π* orbital of the C—C, N—C explaining both the elongation and the red shift. The —CH_2O stretching modes can be used as a good probe for evaluating the bonding configuration around the corresponding atoms and the electronic distribution of the benzene molecule. Hence the 5-chloro-2-((4-chlorophenoxy)methyl)-benzimidazole structure is stabilized by these orbital interactions. The NBO analysis also describes the bonding in terms of the natural hybrid orbital n2(Cl_{28}), which occupy a higher energy orbital (−0.32212 a.u.) with considerable p-character (100.00%) and low occupation number (1.97849 a.u.) and the other n1(Cl_{28}) occupy a lower energy orbital (−0.93930) with p-character (58.96%) and high occupation number (1.99441 a.u.), n2(Cl_{29}), which occupy a higher energy orbital (−0.310652 a.u.) with considerable p-character (100.00%) and low occupation number (1.97933 a.u.) and the other n1(Cl_{29}) occupy a lower energy orbital (−0.92760) with p-character (14.15%) and high occupation number (1.99446 a.u.). Also n1(N_{10}), which occupy a higher energy orbital (−0.261864 a.u.) with considerable p-character (100.00%) and low occupation number (1.60853 a.u.) and the other n1(N_9) occupy a lower energy orbital (−0.35666) with p-character (66.42%) and high occupation number (1.92622 a.u.). Thus, a very close to pure p-type lone pair orbital participates in the electron donation to the σ*(C—C) orbital for n2(Cl_{28}) → σ*(C—C), σ*(C—C) orbital for n2(Cl_{29}) → σ*(C—C) and σ*(N—C) orbital for n1(N_{10}) → σ*(N—C), n1(N_9) → σ*(N—C) interactions in the compound. The results are tabulated in Table S2 as supporting material.

Mulliken charges

The calculation of atomic charges plays an important role in the application of quantum mechanical calculations to molecular systems. Mulliken charges are calculated by determining the electron population of each atom as defined in the basis functions. The charge distributions calculated by the Mulliken [95] and NBO methods for the equilibrium geometry of 5-chloro-2-((4-chlorophenoxy)methyl)-benzimidazole are given in Table S3 as supporting information. The charge distribution on the molecule has an important influence on the vibrational spectra. In 5-chloro-2-((4-chlorophenoxy)methyl)-benzimidazole, the Mulliken atomic charge of the carbon atoms in the neighborhood of C3, C4, C11, C15 become more positive, shows the direction of delocalization and shows that the natural atomic charges are more sensitive to the changes in the molecular structure than Mulliken's net charges. The results are given as supporting material in Fig. S4. Also we done a comparison of Mulliken charges obtained by different basic sets and tabulated it in Table S4 as supporting material in order to assess the sensitivity of the calculated charges to changes in (i) the choice of the basis set; (ii) the choice of the quantum mechanical method. The results are in given graphical form as supporting information in Fig. S5. We have observed a change in the charge distribution by changing different basis sets.

MEP is related to the ED and is a very useful descriptor in understanding sites for electrophilic and nucleophilic reactions as well as hydrogen bonding interactions [96,97]. The electrostatic potential $V(r)$ is also well suited for analyzing processes based on the "recognition" of one molecule by another, as in drug-receptor, and enzyme-substrate interactions, because it is through their potentials that the two species first "see" each other [98,99]. To predict reactive sites of electrophilic and nucleophilic attacks for

Table 2
Second-order perturbation theory analysis of Fock matrix in NBO basis corresponding to the intramolecular bonds of the title compound.

Donor(i)	Type	ED (e)	Acceptor(j)	Type	ED (e)	$E(2)$[a]	$E(j)$–$E(i)$[b]	$F(i, j)$[c]
C1—C2	σ	197.0	C1—C6	σ*	0.02	3.04	1.24	0.06
–	–	–	C2—C3	–	0.02	3.22	1.26	0.06
–	–	–	C3—N10	–	0.03	6.69	1.12	0.08
–	–	–	C6—Cl29	–	0.04	4.54	0.78	0.05
C1—C2	π	1.72	C3—C4	π*	0.48	19.67	0.27	0.07
–	–	–	C5—C6	–	0.36	18.35	0.27	0.07
C1—C6	σ	1.98	C1—C2	σ*	0.01	2.49	1.29	0.05
–	–	–	C2—H7	–	0.01	2.10	1.17	0.04
–	–	–	C5—C6	–	0.02	3.94	1.29	0.06
–	–	–	C5—H8	–	0.01	2.07	1.19	0.04
C1—H27	σ	1.98	C2—C3	σ*	0.02	3.53	1.09	0.06
–	–	–	C5—C6	–	0.02	3.97	1.10	0.06
C2—C3	σ	1.98	C1—C2	σ*	0.01	2.55	1.29	0.05
–	–	–	C1—H27	–	0.01	2.10	1.19	0.05
–	–	–	C3—C4	–	0.04	4.61	1.24	0.07
–	–	–	C3—N10	–	0.03	2.55	1.14	0.05
C2—H7	σ	1.98	C1—C6	σ*	0.02	3.64	1.08	0.06
–	–	–	C3—C4	–	0.04	4.08	1.06	0.06
C3—C4	σ	1.97	C2—C3	σ*	0.02	4.55	1.25	0.07
–	–	–	C2—H7	–	0.01	2.45	1.14	0.05
–	–	–	C4—C5	–	0.02	3.72	1.26	0.06
–	–	–	C5—H8	–	0.01	2.18	1.16	0.05
–	–	–	N10—H26	–	0.02	4.10	1.13	0.06
C3—C4	π	1.60	C1—C2	π*	0.33	19.36	0.28	0.07
–	–	–	C5—C6	–	0.36	20.57	0.27	0.07
–	–	–	N9—C11	–	0.35	13.97	0.25	0.05
C3—N10	σ	1.98	C2—C3	σ*	0.02	2.43	1.37	0.05
–	–	–	C4—C5	–	0.02	2.54	1.38	0.05
–	–	–	C11—C12	–	0.03	3.91	1.22	0.06
C4—C5	σ	1.97	C3—C4	σ*	0.04	3.58	1.22	0.06
–	–	–	C4—N9	–	0.02	2.20	1.13	0.05
–	–	–	C5—C6	–	0.02	3.08	1.27	0.06
–	–	–	C6—Cl29	–	0.04	5.53	0.78	0.06
C4—N10	σ	1.98	C2—C3	σ*	0.02	2.48	1.33	0.05
–	–	–	C4—C5	–	0.02	2.39	1.33	0.05
–	–	–	C11—C12	–	0.03	7.01	1.17	0.08
C5—C6	σ	1.98	C1—C6	σ*	0.02	3.83	1.27	0.06
–	–	–	C4—C5	–	0.02	2.81	1.30	0.05
–	–	–	C4—N9	–	0.02	4.94	1.16	0.07
–	–	–	C5—H8	–	0.01	2.05	1.20	0.04
C5—C6	π	1.73	C1—C2	π*	0.33	19.49	0.29	0.07
–	–	–	C3—C4	–	0.49	16.88	0.28	0.07
C5—H8	σ	1.98	C1—C6	σ*	0.02	4.06	1.06	0.06
–	–	–	C3—C4	–	0.04	4.01	1.04	0.06
C6—Cl29	σ	1.99	C1—C2	σ*	0.01	2.60	1.22	0.05
–	–	–	C4—C5	–	0.02	2.74	1.22	0.05
N9—C11	σ	1.98	C4—C5	σ*	0.02	4.92	1.43	0.08
–	–	–	N10—H26	–	0.02	2.16	1.30	0.05
N9—C11	σ	1.88	C3—C4	σ*	0.49	17.60	0.32	0.08
N10—C11	π	1.99	C2—C3	π*	0.02	4.83	1.39	0.07
N10—H26	σ	1.99	N9—C11	σ*	0.01	2.34	1.23	0.05
C11—C12	σ	1.98	C4—N9	σ*	0.02	2.49	1.12	0.05
–	–	–	C15—O25	–	0.03	2.20	0.98	0.04
C12—H13	σ	1.98	N9—C11	σ*	0.35	3.70	0.54	0.04
–	–	–	N10—C11	–	0.05	2.21	0.96	0.04
C12—H14	π	1.98	N9—C11	π*	0.35	3.70	0.54	0.04
–	–	–	N10—C11	–	0.05	2.21	0.96	0.04
C12—O25	σ	1.99	N9—C11	σ*	0.01	2.92	1.34	0.06
–	–	–	C15—C17	–	0.02	2.33	1.36	0.05
C15—C16	σ	1.98	C15—C17	σ*	0.02	4.36	1.28	0.07
–	–	–	C16—C18	–	0.02	2.74	1.28	0.05
C15—C16	π	1.67	C17—C20	π*	0.32	17.81	0.29	0.06
–	–	–	C18—C22	–	0.38	21.93	0.28	0.07
C15—C17	σ	1.97	C12—O25	σ*	0.01	2.69	0.93	0.05
–	–	–	C15—C16	–	0.03	4.16	1.26	0.07
–	–	–	C16—H19	–	0.01	2.23	1.17	0.05
–	–	–	C17—C20	–	0.01	2.46	1.28	0.05
–	–	–	C20—H24	–	0.01	2.13	1.18	0.05
C16—C18	σ	1.97	C15—C16	σ*	0.03	3.17	1.25	0.06
–	–	–	C15—O25	–	0.03	4.87	1.00	0.06
–	–	–	C18—C22	–	0.02	3.24	1.26	0.06
–	–	–	C22—Cl28	–	0.04	5.23	0.78	0.06
C16—H19	σ	1.98	C15—C17	σ*	0.02	3.81	1.09	0.06
–	–	–	C18—C22	–	0.02	3.53	1.10	0.06

(*continued on next page*)

Table 2 (*continued*)

Donor(*i*)	Type	ED (e)	Acceptor(*j*)	Type	ED (e)	*E*(2)[a]	*E*(*j*)–*E*(*i*)[b]	*F*(*i*, *j*)[c]
C17—C20	σ	1.97	C15—C17	σ*	0.02	2.60	1.26	0.05
–	–	–	C15—O25	–	0.03	3.81	1.00	0.06
–	–	–	C20—C22	–	0.02	3.21	1.26	0.06
–	–	–	C22—Cl28	–	0.04	5.15	0.78	0.06
C17—C20	π	1.70	C15—C16	π*	0.39	21.81	0.27	0.07
–	–	–	C18—C22	–	0.38	18.80	0.27	0.07
C17—H21	σ	1.98	C15—C16	σ*	0.03	4.11	1.08	0.06
–	–	–	C20—C22	–	0.02	3.63	1.08	0.06
C18—C22	σ	1.98	C16—C18	σ*	0.02	2.59	1.29	0.05
–	–	–	C20—C22	–	0.02	3.97	1.28	0.06
–	–	–	C20—H24	–	0.01	1.99	1.20	0.04
C18—C22	π	1.70	C15—C16	π*	0.39	16.56	0.28	0.06
–	–	–	C17—C20	–	0.32	21.01	0.29	0.07
C18—H23	σ	1.98	C15—C16	σ*	0.03	3.64	1.08	0.06
–	–	–	C20—C22	–	0.02	3.95	1.08	0.06
C20—C22	σ	1.98	C17—C20	σ*	0.01	2.56	1.30	0.05
–	–	–	C17—H21	–	0.02	2.13	1.19	0.05
–	–	–	C18—C22	–	0.01	4.00	1.29	0.06
–	–	–	C18—H23	–	0.01	2.07	1.20	0.05
C20—H24	σ	1.98	C15—C17	σ*	0.02	3.62	1.08	0.06
–	–	–	C18—C22	–	0.02	3.84	1.09	0.06
C22—Cl28	σ	1.99	C16—C18	σ*	0.02	2.63	1.22	0.05
–	–	–	C17—C20	σ*	0.01	2.50	1.23	0.05
LP (1)N9	n	1.93	C3—C4	σ*	0.04	5.89	0.87	0.06
–	–	–	N10—C11	–	0.05	10.09	0.76	0.08
LP (1)N10	n	1.61	C3—C4	π*	0.49	33.54	0.29	0.09
–	–	–	N9—C11	–	0.35	50.23	0.27	0.11
LP (1)O25	n	1.96	C15—C16	σ*	0.03	6.11	1.11	74.00
LP (2)O25	n	1.86	C12—H13	σ*	0.02	4.49	0.74	0.05
–	–	–	C12—H14	–	0.02	4.49	0.74	0.05
–	–	–	C15—C16	π*	0.39	26.65	0.33	0.09
LP (1)Cl 28	n	1.99	C18—C22	σ*	0.02	0.95	1.48	0.03
–	–	–	C20—C22	–	0.02	0.94	1.47	0.03
LP (2)Cl28	n	1.98	C18—C22	σ*	0.02	3.06	0.87	0.05
–	–	–	C20—C22	–	0.02	3.06	0.86	0.05
LP (3)Cl28	n	1.95	C18—C22	π*	0.38	9.61	0.31	0.05
LP (1)Cl29	n	1.99	C1—C6	σ*	0.02	0.86	1.46	0.03
–	–	–	C5—C6	–	0.02	0.87	1.49	0.03
LP (2)Cl 29	n	1.98	C1—C6	σ*	0.02	2.92	0.84	0.04
–	–	–	C5—C6	–	0.02	2.93	0.87	0.05
LP (3)Cl29	n	1.95	C5—C6		0.36	9.36	0.32	0.05

[a] E(2) means energy of hyper conjugative interactions (stabilization energy).
[b] Energy difference between donor and acceptor i and j NBO orbitals.
[c] F(i, j) is the Fock matrix element between i and j NBO orbitals.

the investigated molecule, MEP at the B3LYP/6-31G(d,p) optimized geometry was calculated. The negative (red and yellow)[1] regions of MEP were related to electrophilic reactivity and the positive (blue) regions to nucleophilic reactivity (Fig. 4). From the MEP it is evident that the negative charge covers the —CH_2O— group and the positive region is over the methoxyl group. The more electro negativity methoxy makes it the most reactive part in the molecule.

^{1}H NMR spectrum

The experimental spectrum data of 5-chloro-2-((4-chlorophenoxy)methyl)-benzimidazole in DMSO with TMS as internal standard is obtained at 400 MHz and is displayed in Table 3. The absolute isotropic chemical shielding of 5-chloro-2-((4-chlorophenoxy)methyl)-benzimidazole was calculated by B3LYP/GIAO model [100]. Relative chemical shifts were then estimated by using the corresponding TMS shielding: σ_{calc}·(TMS) calculated in advance at the same theoretical level as this paper. Numerical values of chemical shift $\delta_{calc} = \sigma_{calc}$·(TMS) − σ_{calc} together with calculated values of σ_{calc}·(TMS), are reported in Table 3. It could be seen from Table 3 that chemical shift was in agreement with the experimental ^{1}H NMR data. Thus, the results showed that the predicted proton chemical shifts were in good agreement with the experimental data for 5-chloro-2-((4-chlorophenoxy)methyl)-benzimidazole.

Electronic absorption spectra

Electronic transitions are usually classified according to the orbitals engaged or to specific parts of the molecule involved. Common types of electronic transitions in organic compounds are π–π*, n–π* and π*(acceptor)–π(donor). The UV–visible bands in 2-(phenoxymethyl) benzimidazole are observed at 282, 274, 256, 244, 241

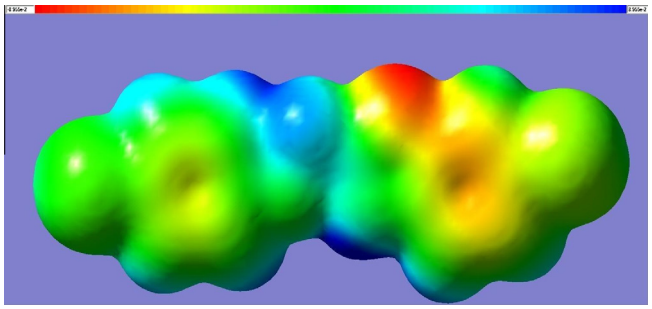

Fig. 4. Molecular electrostatic potential calculated at B3LYP/SDD level.

[1] For interpretation of color in Fig. 4, the reader is referred to the web version of this article.

Table 3
Experimental and calculated ^{1}H NMR parameters (with respect to TMS).

Proton	σ_{TMS}	B3LYP/6-31G	δ_{calc} ($\sigma_{TMS}-\sigma_{calc}$)	Exp. δ_{ppm}
H7	32.7711	25.0012	7.7699	7.623
H8	–	25.1410	7.6301	7.619
H13	–	27.3393	5.4318	5.336
H14	–	27.3398	5.4313	5.336
H19	–	25.8111	6.96	7.096
H21	–	25.3522	7.4189	7.389
H23	–	25.3454	7.4257	7.579
H24	–	25.3384	7.4327	7.558
H26	–	23.2316	9.5395	9.246
H27	–	25.4487	7.3224	7.350

and 240.8 nm. Observed band at 240.8 nm is due to the π–π*. The less intense band centered at 256 nm is due to the partly forbidden n–π* transition from HOMO to LUMO. The more intense band observed at 282 nm belonged to the dipole-allowed π–π* transition.

In order to understand the electronic transitions of 5-chloro-2-((4-chlorophenoxy)methyl)-benzimidazole, TD-DFT calculation on electronic absorption spectrum in vacuum was performed. TD-DFT calculation is capable of describing the spectral features of 5-chloro-2-((4-chlorophenoxy)methyl)-benzimidazole because of the qualitative agreement of line shape and relative strength as compared with experiment. The absorption spectra of organic compounds stem from the ground-to-excited state vibrational transition of electrons. The intense band in the UV range of the electronic absorption spectrum is observed at 282 nm, which is indicating the presence of – OPh entity in the compound. The calculated six lowest-energy transitions of the molecule from TD-DFT method and the observed electronic transitions are listed in Table 4.

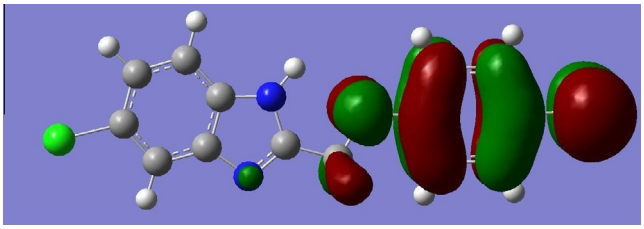

Fig. 5. HOMO plot of 5-chloro-2-((4-chlorophenoxy)methyl)benzimidazole.

From the table the calculated energy transitions are red shifted from the experimental value, because these bands are observed in gas phase without considering the solvent effect.

HOMO and LUMO are the very important parameters for quantum chemistry. The conjugated molecules are characterized by a highest occupied molecular orbital–lowest unoccupied molecular orbital (HOMO–LUMO) separation, which is the result of a significant degree of ICT from the end-capping electron-donor groups to the efficient electron-acceptor groups through π-conjugated path. The strong charge transfer interaction through π-conjugated bridge results in substantial ground state donor–acceptor mixing and the appearance of a charge transfer band in the electronic absorption spectrum. Therefore, an ED transfer occurs from the more aromatic part of the π-conjugated system in the electron-donor side to its electron-withdrawing part. The atomic orbital components of the frontier molecular orbital are shown in Figs. 5 and 6. The HOMO–LUMO energy gap value is found to be 3.916 eV, which is responsible for the bioactive property of the compound 5-chloro-2-((4-chlorophenoxy)methyl)-benzimidazole.

Table 4
Calculated electronic absorption spectrum of 5-chloro-2-((4-chlorophenoxy)methyl)-benzimidazole using TD-DFT/B3LYP/SDD.

Excitation –	CI expansion Coefficient	Energy (eV) –	Wavelength nm	Wavelength Expt. nm	Oscillator Strength (f)
Excited state 1					
73 → 80	0.11094	4.8257	256.92	282	0.1090
74 → 80	0.29439	–	–	–	–
75 → 76	0.56018	–	–	–	–
75 → 77	0.26345	–	–	–	–
Excited state 2					
72 → 78	0.28824	4.9854	248.69	274	0.0295
73 → 76	0.40769	–	–	–	–
73 → 77	−0.27779	–	–	–	–
74 → 76	−0.32885	–	–	–	–
74 → 77	0.18226	–	–	–	–
75 → 77	0.11123	–	–	–	–
Excited state 3					
73 → 76	0.16279	5.0327	246.36	256	0.0820
73 → 77	−0.17278	–	–	–	–
74 → 76	0.53969	–	–	–	–
74 → 77	0.11638	–	–	–	–
75 → 77	0.21674	–	–	–	–
75 → 80	−0.17270	–	–	–	–
Excited state 4					
73 → 76	−0.11699	5.0626	244.90	244	0.0096
74 → 76	−0.10726	–	–	–	–
74 → 77	−0.18373	–	–	–	–
75 → 76	−0.32530	–	–	–	–
75 → 77	0.54186	–	–	–	-
Excited state 5					
73 → 76	−0.44194	5.1293	241.72	241	0.0050
73 → 77	−0.18128	–	–	–	–
74 → 77	0.48871	–	–	–	–
Excited state 6					
73 → 76	0.19995	5.1541	240.55	240.8	0.0400
73 → 77	0.51524	–	–	–	–
74 → 77	0.33644	–	–	–	–
75 → 80	−0.14400	–	–	–	–

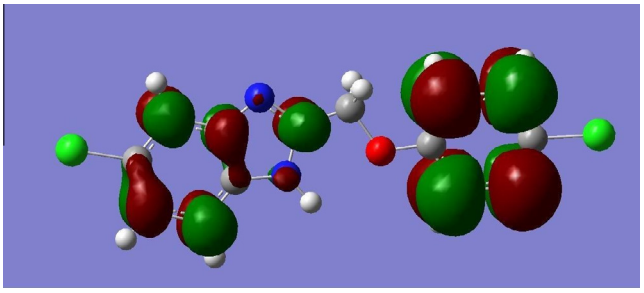

Fig. 6. LUMO plot of 5-chloro-2-((4-chlorophenoxy)methyl)benzimidazole.

Conclusion

The present investigation thoroughly reports the vibrational spectra, both infrared and Raman of the title compound. All the vibrational bands observed in the FT-IR and FT-Raman spectra of the title compound are assigned to various modes of vibration. Most of the modes have wave numbers in the range suggested by previous assignments found in literature in the case of related molecules. The simultaneous activation of the phenyl ring stretching modes in the IR and Raman spectra can be interpreted as the evidence of intra molecular charge transfer between the donor and the acceptor group via conjugated ring path, which is responsible for hyperpolarizability enhancement, leading to non-linear optical activity. The NBO analysis confirms the ICT formed by the orbital overlap between n (Cl) and σ^*(C—C), n(N) and σ^*(N—C). A very close to pure p-type lone pair orbital participates in the electron donation to the σ^*(C—C) orbital for n2(Cl28) → σ^*(C—C), σ^*(C—C) orbital for n2(Cl29) → σ^*(C—C) and σ^*(N—C) orbital for n1(N10) → σ^*(N—C), n1(N9) → σ^*(N—C) interaction in the molecule. Overall, the TD-DFT calculations on the molecule provided deep insight into their electronic structures and properties. GIAO NMR calculations provided chemical shift values that were in excellent agreement with experimental data. In addition, the calculated UV–Vis results are all in good agreement with the experimental data. The lowering of HOMO–LUMO band gap supports bioactive property of the molecule. MEP predicts the most reactive part in the molecule.

Acknowledgments

SA and IY would like to thank the Research Fund of Ankara University (Grant No. 12B3336002) for the financial support in this research. The authors are thankful to University of Antwerp for access to the university's CalcUA Supercomputer Cluster.

Appendix A. Supplementary material

Supplementary data associated with this article can be found, in the online version, at http://dx.doi.org/10.1016/j.saa.2013.11.025.

References

[1] K.F. Ansari, C. Lal, Eur. J. Med. Chem. 44 (2009) 4028–4033.
[2] G.A. Kilcigil, N. Altanlar, Il Farmaco 58 (2003) 1345–1350.
[3] S. Ozden, D. Atabey, S. Yildiz, H. Goker, Bioorg Med. Chem. 13 (2005) 1587–1597.
[4] M. Andrzejewska, L.Y. Mulia, R.C. Rivera, A. Tapia, L. Vilpo, J. Vilpo, Z. Kazimierczuk, Eur. J. Med. Chem. 37 (2002) 973–978.
[5] D.V. LaBarber, S.B. Skibo, Bioorg. Med. Chem. 13 (2005) 387–395.
[6] H. Kucukbay, R. Durmaz, E. Orhan, S. Gunal, Il Farmaco 58 (2003) 431–437.
[7] N.M.A. Atabay, B. Dulger, F. Gucin, Eur. J. Med. Chem. 38 (2003) 875–881.
[8] G.N. Vazquez, R. Cedillo, A.H. Campos, L. Yepez, F.H. Luis, J. Valdez, R. Morales, R. Cortes, M. Hernandez, R. Castillo, Bioorg. Med.Chem. Lett. 11 (2001) 187–190.
[9] J. Cheng, J. Xie, X. Luo, Bioorg. Med. Chem. Lett. 15 (2005) 267–269.
[10] S.M. Sondhi, R. Rani, J. Singh, P. Roy, S.K. Agarwal, A.K. Saxena, Bioorg. Med. Chem. Lett. 20 (2010) 2306–2310.
[11] R.L. Lombardy, F.A. Tanious, K. Ramachandran, R.R. Tidwell, W.D. Wilson, J. Med. Chem. 39 (1996) 1452–1462.
[12] M.J. Tebbe, W.A. Spitzer, F. Victor, S.C. Miller, C.C. Lee, T.R. Sattelberg Sr., E. McKinney, J.C. Tang, J. Med. Chem. 40 (1997) 3937–3946.
[13] A.R. Porcari, R.V. Devivar, L.S. Kucera, J.C. Drach, L.B. Townsend, J. Med. Chem. 41 (1998) 1252–1262.
[14] T.C. Kuhler, M. Swanson, V. Shcherbuchin, H. Larsson, B. Mellgard, J.E. Sjostrom, J. Med. Chem. 41 (1998) 1777–1788.
[15] I. Tapia, L. Alonso-Cires, P.L. Lopez-Tudanca, R. Mosquera, L. Labeaga, A. Innerarity, A. Orjales, J. Med. Chem. 42 (1999) 2870–2880.
[16] J.J. Chen, Y. Wie, J.C. Drach, J.C. Townsend, J. Med. Chem. 43 (2000) 2449–2456.
[17] A.W. White, R. Almassy, A.H. Calvert, N.J. Curtin, R.J. Griffin, Z. Hostomsky, K. Maegley, D.R. Newell, S. Srinivasan, B.T. Golding, J. Med. Chem. 43 (2000) 4084–4097.
[18] W. Roth, D. Spangenberg, C. Janzen, A. Westphal, M. Schmitt, Chem. Phys. 248 (1999) 17–25.
[19] E. Jalviste, A. Treshchalov, Chem. Phys. 172 (1993) 325–338.
[20] B.C. Bishop, E.T.J. Chelton, A.S. Jones, Biochem. Pharmacol. 13 (1964) 751–754.
[21] N.S. Habib, R. Soliman, F.A. Ashoura, M. El-Taiebi, Pharmazie 55 (1997) 746–749.
[22] M. Tuncbilek, H. Goker, R. Ertan, R. Eryigit, E. Kendi, E. Altanlar, Arch. Pharm. 330 (1997) 372–376.
[23] H. Goker, C. Kus, D.W. Boykin, S. Yildiz, N. Altanlar, Arch. Pharm. 334 (2001) 148–152.
[24] H. Goker, C. Kus, D.W. Boykin, S. Yildiz, N. Altanlar, Bioorg. Med. Chem. 10 (2002) 2589–2596.
[25] N.S. Pawar, D.S. Dalal, S.R. Shimpi, P.P. Mahulikan, Eur. J. Pharm. Sci. 21 (2004) 115–118.
[26] B.G. Mohammad, M.A. Hussein, A.A. Abdel-Alim, M. Hashem, Arch. Pharm. Res. 29 (2006) 26–33.
[27] S.D. Vaidya, B.V.S. Kumar, R.V. Kumar, U.N. Bhise, U.C. Mashelkar, J. Heterocycl. Chem. 44 (2007) 685–691.
[28] W. Huo, F. Jian, Z. Zhengzhi, Biolog. Trace Elem. Res. 64 (1998) 27–35.
[29] J. Cheng, J. Xie, X. Luo, Bioorg. Med. Chem. Lett. 15 (2005) 267–269.
[30] Y. He, J. Yang, B. Wu, L. Risen, E.E. Swayze, Bioorg. Med. Chem. Lett. 14 (2004) 1217–1220.
[31] M.A. Ismail, R. Brun, T. Wenzler, F.A. Tanious, D. Wilson, D.W. Boykin, Bioorg. Med. Chem. 12 (2004) 5405–5413.
[32] H. Nakano, T. Inoue, N. Kawasaki, H. Miyataka, H. Matsumoto, T. Taguchi, N. Inagaki, H. Nasai, T. Satoh, Bioorg. Med. Chem. 8 (2000) 373–380.
[33] R. Marquis, J. Sheng, T. Nguyen, J. Baldeck, J. Olsson, Arch. Oral. Biol. 51 (2006) 1015–1023.
[34] A.T. Mavrova, K. Anichina, D. Vuchev, J. Tsenov, P. Denkova, M. Kondeva, M. Micheva, Eur. J. Med. Chem. 41 (2006) 1412–1420.
[35] S.O. Podunavac-Kuzmonovic, L.M. Leovac, N.V. Perisicjanjic, J. Rogan, J. Balaz, J. Serb, Chem. Soc. 64 (1999) 381–384.
[36] M. Boiani, M. Gonzalez, Mini Rev. Med. Chem. 5 (2005) 409–424.
[37] I. Yildiz-Oren, I. Yalcin, E. Aki-Sener, N. Ucarturk, Eur. J. Med. Chem. 39 (2004) 291–298.
[38] M.A. Philips, J. Chem. Soc. (1928) 2393–2399.
[39] Gaussian 09, Revision B.01, M.J. Frisch, G.W. Trucks, H.B. Schlegel, G.E. Scuseria, M.A. Robb, J.R. Cheeseman, G. Scalmani, V. Barone, B. Mennucci, G.A. Petersson, H. Nakatsuji, M. Caricato, X. Li, H.P. Hratchian, A.F. Izmaylov, J. Bloino, G. Zheng, J.L. Sonnenberg, M. Hada, M. Ehara, K. Toyota, R. Fukuda, J. Hasegawa, M. Ishida, T. Nakajima, Y. Honda, O. Kitao, H. Nakai, T. Vreven, J.A. Montgomery, Jr., J.E. Peralta, F. Ogliaro, M. Bearpark, J.J. Heyd, E. Brothers, K.N. Kudin, V.N. Staroverov, T. Keith, R. Kobayashi, J. Normand, K. Raghavachari, A. Rendell, J.C. Burant, S.S. Iyengar, J. Tomasi, M. Cossi, N. Rega, J.M. Millam, M. Klene, J.E. Knox, J.B. Cross, V. Bakken, C. Adamo, J. Jaramillo, R. Gomperts, R.E. Stratmann, O. Yazyev, A.J. Austin, R. Cammi, C. Pomelli, J.W. Ochterski, R.L. Martin, K. Morokuma, V.G. Zakrzewski, G.A. Voth, P. Salvador, J.J. Dannenberg, S. Dapprich, A.D. Daniels, O. Farkas, J.B. Foresman, J.V. Ortiz, J. Cioslowski, D.J. Fox, Gaussian Inc., Wallingford CT, 2010.
[40] J.B. Foresman, in: E. Frisch (Ed.), Exploring Chemistry with Electronic Structure Methods: A Guide to Using Gaussian, Gaussian, Inc., Pittsburg, PA, 1996.
[41] P.J. Hay, W.R. Wadt, J. Chem. Phys. 82 (1985) 270–283.
[42] J. Zhao, Y. Zhang, L. Zhu, J. Mol. Struct. Theochem. 671 (2004) 179–187.
[43] GaussView, Version 5, Roy Dennington, Todd Keith and John Millam, Semichem Inc., Shawnee Mission KS, 2009.
[44] J.M.L. Martin, C. Van Alsenoy, GAR2PED, A Program to Obtain a Potential Energy Distribution from a Gaussian Archive Record, University of Antwerp, Belgium, 2007.
[45] P.L. Anto, C.Y. Panicker, H.T. Varghese, D. Philip, O. Temiz-Arpaci, B. Tekiner-Gulbas, I. Yildiz, Spectrochim. Acta Part A 67 (2007) 744–749.
[46] R. Saxena, L.D. Kandpal, G.N. Mathur, J. Polym. Sci. A: Polym. Chem. 40 (2002) 3959–3966.
[47] R.M. Silverstein, G.C. Bassler, T.C. Morril, Spectrometric Identification of Organic Compounds, fifth ed., John Wiley and Sons Inc., Singapore, 1991.
[48] K Nakamoto, Infrared and Raman spectrum of Inorganic and Coordination Compounds, fifth ed., John Wiley and Sons Inc., New York, 1997.

[49] J.B. Bhagyasree, H.T. Varghese, C.Y. Panicker, J. Samuel, C. Van Alsenoy, K. Bolelli, I. Yildiz, E. Aki, Spectrochim. Acta 102 (2013) 99–113.
[50] N.B. Colthup, L.H. Daly, S.E. Wiberly, Introduction to Infrared and Raman Spectroscopy, second ed., Academic Press, New York, 1975.
[51] N. Sandhyarani, G. Skanth, S. Berchmanns, V. Yegnaraman, T. Pradeep, J. Colloid Interface Sci. 209 (1999) 154.
[52] K. Malek, A. Puc, G. Schroeder, V.I. Rybachenko, L.M. Proniewich, Chem. Phys. 327 (2006) 439–451.
[53] N.P.G. Roeges, A Guide to the Complete Interpretation of Infrared Spectra of Organic Structures, John Wiley and Sons Inc., New York, 1994.
[54] G. Socrates, Infrared Characteristic Group Frequencies, John Wiley and Sons, New York, 1981.
[55] A. Spire, M. Barthes, H. Kallouai, G. De Nunzio, Physics D 137 (2000) 392–396.
[56] R. Minitha, Y.S. Mary, H.T. Varghese, C.Y. Panicker, R. Ravindran, K. Raju, V.M. Nair, J. Mol. Struct. 985 (2011) 316–322.
[57] C.Y. Panicker, H.T. Varghese, V.S. Madhavan, S. Mathew, J. Vinsova, C. Van Alsenoy, Y.S. Mary, Y.S. Mary, J. Raman Spectrosc. 40 (2009) 2176–2186.
[58] M.S. Kim, M.K. Kim, C.J. Lee, Y.M. Jung, M.S. Lee, Bull. Korean Chem. Soc. 30 (2009) 2930–2934.
[59] A. Bigotto, B. Pergolese, J. Raman Spectrosc. 32 (2001) 953–959.
[60] C. Lee, W. Yang, R.G. Parr, Phys. Rev. 37B (1998) 785–789.
[61] E.F. Mooney, Spectrochim. Acta 20 (1964) 1021–1032.
[62] E.F. Mooney, Spectrochim. Acta 19 (6) (1963) 877–887.
[63] N. Sundaraganesan, C. Meganathan, B.D. Joshua, P. Mani, A. Jayaprakash, Spectrochim. Acta 71A (2008) 1134–1139.
[64] G. Varsanyi, Assignments of Vibrational Spectra of Seven Hundred Benzene derivatives, Wiley, New York, 1974.
[65] P. Pazdera, H. Divisova, H. Havilsova, P. Borek, Molecules 5 (2000) 189–194.
[66] P. Pazdera, H. Divisova, H. Havilsova, P. Borek, Molecules 5 (2000) 1166–1174.
[67] H.T. Varghese, C.Y. Panicker, D. Philip, P. Pazdera, Spectrochim. Acta 67A (2007) 1055–1059.
[68] H. Arslan, U. Florke, N. Kulcu, G. Binzet, Spectrochim. Acta 68A (2007) 1347–1355.
[69] W.O. George, P.S. Mcintyre, Infrared Spectroscopy, first ed., John Wiley and Sons, Chichester, 1987.
[70] M.A. Palafox, V.K. Rastogi, L. Mittal, Int. J. Quant. Chem. 94 (2003) 189–204.
[71] M. Kurt, J. Raman Spectrosc. 40 (1) (2009) 67–75.
[72] A. Raj, Y.S. Mary, C.Y. Panicker, H.T. Varghese, K. Raju, Spectrochim. Acta 113 (2013) 23–36.
[73] M. Kaur, Y.S. Mary, H.T. Varghese, C.Y. Panicker, H.S. Yathirajan, M.S. Siddegowda, C. Van Alsenoy, Spectrochim. Acta 98 (2012) 91–99.
[74] V.S. Madhavan, Y.S. Mary, H.T. Varghese, C.Y. Panicker, S. Mathew, C. Van Alsenoy, J. Vinsova, Spectrochim. Acta 89 (2012) 308–316.
[75] T. Joseph, H.T. Varghese, C.Y. Panicker, T. Thiemann, K. Viswanathan, C. Van Alsenoy, J. Mol. Struct. 1005 (2011) 17–24.
[76] Y.S. Mary, C.Y. Panicker, H.T. Varghese, K. Raju, T.E. Bolelli, I. Yildiz, C.M. Granadeiro, H.I.S. Nogueira, J. Mol. Struct. 994 (2011) 223–231.
[77] J Coates, in: R.A. Meyers (Ed.), Interpretation of Infrared Spectra, A Practical Approach, John Wiley and Sons Inc., Chichester, 2000.
[78] C.Y. Panicker, H.T. Varghese, K.R. Ambujakshan, S. Mathew, S. Ganguli, A.K. Nanda, C. Van Alsenoy, Y.S. Mary, J. Mol. Struct. 963 (2010) 137–144.
[79] K.R. Ambujakshan, V.S. Madhavan, H.T. Varghese, C.Y. Panicker, O. Temiz-Arpaci, B. Tekiner-Gulbas, I. Yildiz, Spectrochim. Acta Part A 69 (2008) 782–788.
[80] A. Lifshitz, C. Tamburu, A. Suslensky, F. Dubnikova, J. Phys. Chem. A 110 (2006) 4607–4613.
[81] J. Chowdhury, J. Sarkar, R. De, M. Ghosh, G.B. Talapatra, Chem. Phys. 330 (2006) 172–183.
[82] J. Sarkar, J. Chowdhury, M. Ghosh, R. De, G.B. Talapatra, J. Phys. Chem. 109B (2005) 22536–22544.
[83] P. Purkayastha, N. Chattopadhyay, Phys. Chem. Chem. Phys. 2 (2000) 203–210.
[84] P. Sykes, A Guide Book to Mechanism in Organic Chemistry, sixth ed., Pearson Education, India, 2004.
[85] D.K. Geiger, H.C. Geiger, L. Williams, B.C. Noll, Acta Cryst. E68 (2012). o420-o420.
[86] M. Sekerci, Y. Atalay, F. Yakuphanoglu, D. Ava, A. Basoglu, Spectrochim. Acta 67 (2007) 503–508.
[87] A. Unal, B. Eren, Spectrochim. Acta 114 (2013) 129–136.
[88] Y.R. Shen, The Principles of Nonlinear Optics, Wiley, New York, 1984.
[89] P.V. Kolinsky, Opt. Eng. 31 (1992) 1676–1684.
[90] D.F. Eaton, Science 25 (1991) 281–287.
[91] D.A. Kleinman, Phys. Rev. 126 (1962) 1977–1979.
[92] L.N. Kuleshova, M.Y. Antipin, V.N. Khrustalev, D.V. Gusev, G.V. Grintselev-Knyazev, E.S. Bobrikova, Cryst. Reports 48 (2003) 594–601.
[93] M. Adant, M. Dupuis, J.L. Bredas, Int. J. Quant. Chem. 56 (1995) 497–507.
[94] NBO Version 3.1, E.D. Glendening, A.E. Reed, J.E. Carpenter, F. Weinhold.
[95] R.S. Mulliken, J. Chem. Phys. 23 (1955) 1833–1840.
[96] E. Scrocco, J. Tomasi, Adv. Quant. Chem. 103 (1978) 115–193.
[97] F.J. Luque, J.M. Lopez, M. Orozco, Theor. Chem. Acc. 103 (2000) 343–345.
[98] P. Politzer, J.S. Murray, in: D.L. Beveridge, R. Lavery (Eds.), Theoretical Biochemistry and Molecular Biophysics: A Comprehensive Survey, Protein, vol. 2, Adenine Press, Schenectady, NY, 1991 (Chapter 13).
[99] E. Scrocco, J. Tomasi, Top. Curr. Chem. 42 (1973) 95–170.
[100] K. Wolinski, J.F. Hinton, P. Pulay, J. Am. Chem. Soc. 112 (1990) 8251–8260.